

this level is forbidden and is inconsistent with the allowed $\log ft$ measured in the present experiment.

ACKNOWLEDGMENTS

We are indebted to P. Richards and J. A. Baronosky of the Applied Science Department for the preparation

of the Mg^{28} samples used in this work. We also wish to thank C. Chasman for the loan of a high-resolution 30-cm³ Ge(Li) detector which had been fabricated at Brookhaven by H. Kraner. The 6-mm-thick $\times \frac{3}{8}$ -in.-diam NaI(Tl) scintillator was kindly lent to us by J. Cumming.

Study of Nuclear States in ^{60}Ni by Inelastic Electron Scattering

Y. TORIZUKA, Y. KOJIMA, M. OYAMADA, K. NAKAHARA, K. SUGIYAMA, T. TERASAWA, K. ITOH,
A. YAMAGUCHI, AND M. KIMURA

Laboratory of Nuclear Science, Tohoku University, Sendai, Japan

(Received 27 September 1968; revised manuscript received 24 February 1969)

Inelastic scattering of electrons from ^{60}Ni was studied with an over-all energy resolution of 0.1% by the use of 183- and 250-MeV electron beams from the Tohoku 300-MeV linear accelerator. Peaks were found at 1.33 (2^+), 2.16 (2^+), 2.50 (4^+), 3.13 (4^+), 3.67 (4^+), 4.04 (3^-), 4.85 (2^+ , 4^+), 5.05 (4^+ , 6^+), 6.20 (3^-), 6.85 (2^+ , 5^-), and 7.05 MeV (3^-). The data were analyzed in Born approximation, using the Helm model to determine multipolarities and reduced transition probabilities. Distorted-wave calculations were also carried out for the 1.33-, 2.50-, and 4.04-MeV states. A striking feature of the present study is the discovery of the collective ($G=11$) 6^+ state at 5.05 MeV. The energies and transition probabilities of low-lying states were compared with the predictions of a recently developed theory based on the shell model.

I. INTRODUCTION

A NUMBER of studies to investigate the nuclear structure of ^{60}Ni have been performed by inelastic scattering, including (e, e'),^{1,2} (p, p'),³⁻⁶ and (α, α')⁷⁻⁹ reactions. When the projectile is an electron, it is well known that the nuclear states are excited by the electromagnetic interaction, which is well understood, and which leads to precise determination of parameters,¹⁰⁻¹² i.e., the spin, parity, and

reduced radiative transition probability. These parameters have been also extracted from inelastic scattering experiments using strongly interacting particles. Thus, it is interesting to compare the results of inelastic electron scattering with the results using other particles.

Inelastic electron scattering from ^{60}Ni was first studied at Stanford using incident electrons of 183 MeV. Recently, very precise measurements of the (e, e') reaction of ^{60}Ni were made at Yale,² where the energy resolution of the spectrum of the scattered electrons was 130 keV. Unfortunately, Duguay *et al.*² missed many excitations because of additional background due to instrumental scattering. The present paper reports the results of inelastic scattering of 183- and 250-MeV electrons from ^{60}Ni . The present experiments have better energy resolution than the previous (e, e') reaction at 183-MeV at Stanford.

Very recently, detailed shell-model calculations¹³⁻¹⁶ were performed for the Ni isotopes, so comparison of the present experimental results with the theoretical predictions can be made for the energies and the

¹ H. Crannell, R. Helm, H. Kendall, J. Oeser, and M. Yearian, *Phys. Rev.* **123**, 923 (1961).

² M. A. Duguay, C. K. Bockelman, T. H. Curtis, and R. A. Eisenstein, *Phys. Rev.* **163**, 1259 (1967).

³ M. Koike, K. Matsuda, I. Nonaka, Y. Saji, K. Yagi, H. Ejiri, Y. Ishizaki, Y. Nakajima, and E. Tanaka, *J. Phys. Soc. Japan* **21**, 2103 (1966).

⁴ S. F. Eccles, H. F. Lutz, and V. A. Madsen, *Phys. Rev.* **141**, 1067 (1966).

⁵ R. Ballini, A. G. Blair, N. Cindro, J. Delaunay, and J. P. Fouan, *Nucl. Phys.* **A111**, 147 (1968).

⁶ M. P. Fricke and G. R. Satchler, *Phys. Rev.* **139**, B567 (1965).

⁷ O. N. Jarvis, B. G. Harvey, D. L. Hendrie, and J. Mahoney, *Nucl. Phys.* **A102**, 625 (1967).

⁸ H. W. Broek, *Phys. Rev.* **130**, 1914 (1963).

⁹ I. Kumabe, H. Ogata, S. Tomita, M. Inoue, and Y. Okuma, *Phys. Letters* **17**, 45 (1965).

¹⁰ W. C. Barber, *Ann. Rev. Nucl. Sci.* **12**, 1 (1962).

¹¹ R. H. Hofstadter, *Rev. Mod. Phys.* **28**, 214 (1956).

¹² T. deForest and J. D. Walecka, *Advan. Phys.* **15**, 1 (1966).

¹³ S. Cohen, R. D. Lawson, M. H. Macfarlane, S. P. Pandya, and M. Soga, *Phys. Rev.* **160**, 903 (1967).

¹⁴ N. Auerbach, *Phys. Rev.* **163**, 1203 (1967).

¹⁵ L. S. Hsu and J. B. French, *Phys. Letters* **19**, 135 (1965).

¹⁶ L. S. Hsu, *Nucl. Phys.* **A96**, 624 (1967).

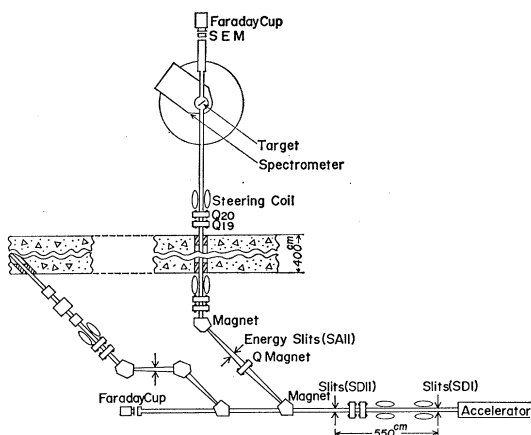


FIG. 1. Outline of the beam transport system in the facility of the Tohoku 300-MeV electron linear accelerator.

reduced transition probabilities of the low-lying states in ^{60}Ni .

II. EXPERIMENTAL METHOD AND RESULTS

The experiments were performed by using the electron beam of the Tohoku 300-MeV linear accelerator,¹⁷ which is able to accelerate electrons to energies between 20 and 300 MeV. The primary beam of the machine had a spread in energy of $\pm 1.0\%$. The quality of the beam was improved by the use of the beam analyzing system¹⁷ shown in Fig. 1. After leaving the end of the accelerator, the electron beam passes through a water-cooled copper-slit system (SD I and

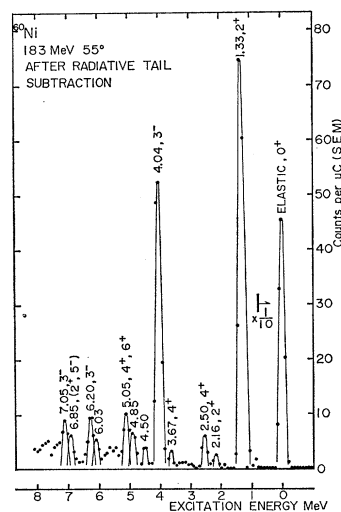


FIG. 2. ^{60}Ni spectrum observed by the use of a 12-channel detector ladder. The incident energy is 183 MeV and the scattering angle is 55° . Close-lying peaks are separated by a fitting procedure using the shape of the elastic peak. The radiative effects were corrected by an unfolding procedure developed by Crannell (see Ref. 21).

¹⁷ Manufactured by Mitsubishi Electric Corp., Tokyo.

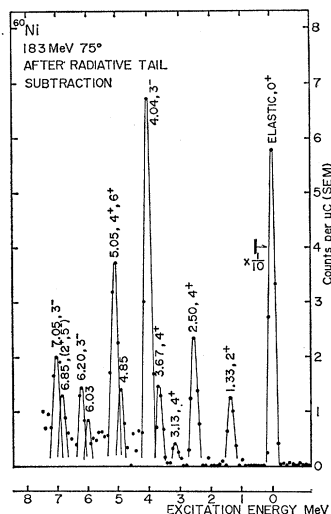


FIG. 3. ^{60}Ni spectrum observed in a 12-channel detector system. The incident energy is 183 MeV and the scattering angle is 75° . See caption to Fig. 2.

SD II) designed to fix the direction and the location of the beam. The nondispersive achromatic magnetic analyzing system consists of a quadrupole magnet between two bending magnets, giving an orbital radius of 130 cm. For the present experiment the slit SA II was adjusted to give a 0.05% spread in energy. The available average current of the analyzed beam was about $1 \mu\text{A}$. The beam was focused to a diameter of 3 mm at the target position by a pair of quadrupole magnets (Q19 and Q20). After passing through the target, the beam was monitored by a secondary emission monitor (SEM) which was calibrated for each experiment against a Faraday cup. The position of the beam spot was monitored by the use of two thin BeO plates viewed by closed-circuit television. One of these was placed at the target position and the other in front of the window of the SEM. The target was a

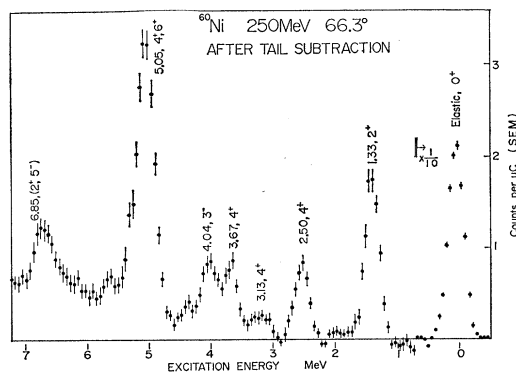


FIG. 4. ^{60}Ni spectrum observed by the use of a 33-channel detector system. The incident energy is 250 MeV and the scattering angle is 66.3° . The length of the vertical line shows the statistical error. The radiative effects were corrected with the method of Crannell.

TABLE I. Inelastic form factors for ^{60}Ni at the incident energy of 183 MeV.

E_x (MeV)	J^π	35°	45°	55°	$10^4 F $ 65°	75°	85°	95°
1.33	2 ⁺	15.8±0.9	19.5±0.10	14.7±0.71	4.16±0.17	0.58±0.11	0.55±0.22	1.22±0.13
2.16	2 ⁺	0.83±0.50	0.50±0.15	0.43±0.12	0.023±0.06	0.045±0.03	0.038±0.01	
2.50	4 ⁺		0.70±0.17	1.18±0.13	1.35±0.13	1.60±0.28	1.14±0.24	0.47±0.12
3.13	4 ⁺		0.20±0.14	0.23±0.12	0.37±0.07	0.37±0.08	0.40±0.08	
3.67	4 ⁺	0.18±0.14	0.24±0.07	0.62±0.12	0.69±0.07	0.89±0.19	1.03±0.24	0.41±0.12
4.04	3 ⁻	4.25±0.17	8.48±0.24	10.3±0.05	7.97±0.19	4.58±0.32	2.35±0.21	0.49±0.12
4.85	(2 ⁺ , 4 ⁺)	1.18±0.23	1.70±0.34	1.16±0.23	0.90±0.11	0.73±0.13	0.64±0.12	0.33±0.09
5.05	4 ⁺ , 6 ⁺		0.82±0.08	1.4±0.13	1.91±0.18	2.29±0.24	2.46±0.22	2.19±0.21
5.05	6 ⁺				0.22±0.18	0.50±0.24	1.10±0.20	
6.20	3 ⁻	1.29±0.15	1.45±0.08	1.78±0.17	1.35±0.14	0.92±0.14	0.50±0.10	0.44±0.18
6.85	(2 ⁺ , 5 ⁻)	0.83±0.12	1.21±0.07	1.20±0.15	1.25±0.12	0.82±0.13	0.84±0.13	0.78±0.13
7.05	3 ⁻	1.04±0.12	1.33±0.08	1.49±0.14	1.21±0.13	1.24±0.16	0.70±0.13	0.53±0.10

thin foil (43.9 mg/cm²) of ^{60}Ni enriched to 97.8% purity.¹⁸ The scattered electrons were deflected by the double-focusing magnet^{17,19} ($r_0=100$ cm, $\theta=169.7^\circ$) and detected with a 12-channel detector system. Later the number of channels was increased to 33, and inelastic scattering of 250-MeV electrons was measured with the new system. Each channel consists of three lithium-drifted silicon detectors ($2\times 1\times 10$ mm), two of which operate as a counter telescope, and the other is kept as a spare. Fast coincidence circuits were not used because a solid-state detector is insensitive to neutron background unlike a plastic scintillator. The slow coincidences were handled by a computer system. The energy bin defined by each channel was 0.05%. The ranges of energy covered by the 12- and 33-channel systems were 1.2 and 3.3% wide, respectively. The location of the counter system can be moved stepwise along the focal plane. Each step corresponds to the 0.05 and 0.025% shifts in energy in 12- and 33-channel systems, respectively. The data collection was performed by a TOSBAC-3400 computer system,²⁰ enabling a spectrum of the scattered electrons to be immediately displayed on an oscilloscope.

Inelastic scattering spectra for ^{60}Ni are shown in Figs. 2-4. The energies and angles, 55° and 183 MeV, 75° and 183 MeV, and 66.3° and 250 MeV are chosen to obtain values of the momentum transfer favorable for 2⁺, 4⁺, and 6⁺ states, respectively. The usual radiative corrections were made using the method of Crannell.²¹ It can be seen in Figs. 2-4 that many well-separated excited states were obtained in the energy region below particle emission threshold. The full width at half-maximum of each peak was about 0.1%, as was expected from the experimental conditions. The uncertainty in determination of the excitation energy was estimated to be ± 100 keV. Absolute

cross sections of inelastic scattering were determined by comparison with those of elastic scattering from ^{12}C .

The Coulomb form factor for inelastic scattering is defined by the relation

$$d\sigma/d\Omega = \sigma_{\text{Mott}} |F(EL, q)|^2, \quad (1)$$

where $\sigma_{\text{Mott}} = (Ze^2/2E_0)^2 \cos^2(\frac{1}{2}\theta)/\sin^4(\frac{1}{2}\theta)$ is the Mott cross section for elastic scattering through an angle θ , of an electron of energy E_0 , from a point, spinless nucleus without recoil. This notation EL means an electric multipole transition of order L . The data were analyzed using the phenomenological model described by Helm²² in the Born approximation. In this case, the inelastic form factor becomes

$$|F(EL, q)|^2 = \beta_L j_L^2(qR) \exp(-q^2 g^2). \quad (2)$$

Here, R and g are spatial parameters of the transition charge density, q is momentum transfer, and β_L measures the strength of the transition and is obtained by normalization to the experimental data. The value of qR is corrected for the change of wavelength of the incident electron when it passes through the nucleus.²² This correction factor is $\gamma = (1 + 3Z\alpha/2k_0R)$, where $k_0 = E_0/\hbar c$ and α is the fine structure constant.

In order that all the experimental data may be compared with a single theoretical curve, the data of 250 MeV were normalized to those of 183 MeV by the use of the correction factor γ , i.e., $|F|^2$ was plotted against $q' = q[\gamma(250 \text{ MeV})/\gamma(180 \text{ MeV})]$.

The points obtained for values of q between 0.5 and 1.6 F^{-1} for each excitation are shown in Figs. 5-9. A noticeable feature of the form factors is the appearance of the minimum which is clearly seen for the 1.33- and 4.04-MeV transitions in the vicinity of $q=1.25$ and 1.45 F^{-1} , respectively. The values of the form factors which were obtained from the present experiment are listed in Tables I and II. A com-

¹⁸ Supplied from Oak Ridge National Laboratory.

¹⁹ M. Sakai, Nucl. Instr. Methods **8**, 61 (1960).

²⁰ Manufactured by Toshiba Electric Corp.

²¹ H. Crannell, Phys. Rev. **148**, 1107 (1966).

²² R. Helm, Phys. Rev. **104**, 1466 (1956).

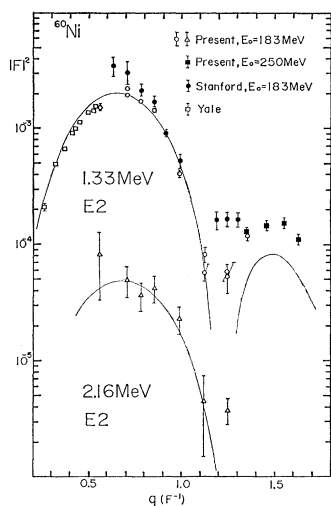


FIG. 5. Experimental $|F|^2$ versus q for the 1.33- and 2.16-MeV excitations in ^{60}Ni . Solid curves are reproduced using Eq. (2) in the text. The experimental data of Stanford and Yale for 1.33-MeV level are also plotted for comparisons.

parison of the predictions of Eq. (2), using the selected L value, with the present data is shown in Figs. 5–9. A better fit to the data is achieved by adjusting R and keeping a fixed value for $g=0.95 F$. The 5.05-MeV peak corresponds to the well-known 4^+ state, however the q dependence of $|F|^2$ shows anomalous behavior which does not fit the prediction of Eq. (2). As can be seen in Fig. 4, the most prominent peaks are observed at 1.33 and 5.05 MeV, the former corresponds to that of the second maximum of $|F|^2$ for the 2^+ state, and the latter may be that of a higher multipole state than $L=4$. After subtraction of the 4^+ component, which is estimated by the use of Eq.

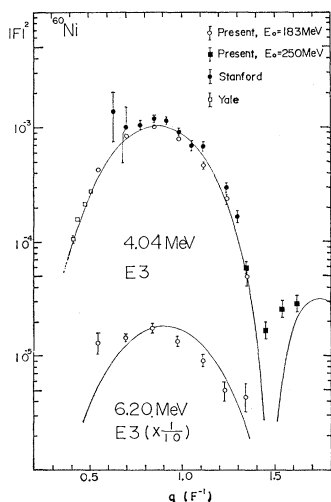


FIG. 6. Experimental $|F|^2$ versus q for the 4.04- and 6.20-MeV excitations. See caption to Fig. 5.

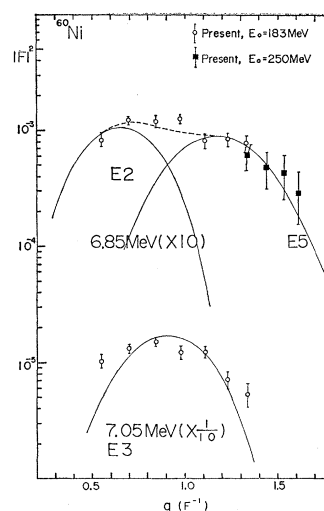


FIG. 7. Experimental $|F|^2$ versus q for the 6.85- and 7.05-MeV excitations. The $|F|^2$ of 6.85-MeV excitation were decomposed tentatively to $E2$ and $E5$ components using the theoretical curves predicted by Eq. (2) in the text.

(2), from the measured $|F|^2$ of the 5.05-MeV peak, the remainder is shown in Fig. 10. The data compare favorably with the theoretical curve corresponding to a 6^+ state. The 4.85- and 6.85-MeV peaks are also doublets which may consist of $(2^+, 4^+)$ and $(2^+, 5^-)$ states, respectively, as shown in Figs. 9 and 7. The spins and parities assigned by the present study for each transition are given in Table III. Those states which have uncertain assignments are given in parentheses.

The value of β_L leads to a reduced transition probability from the ground state to the excited state

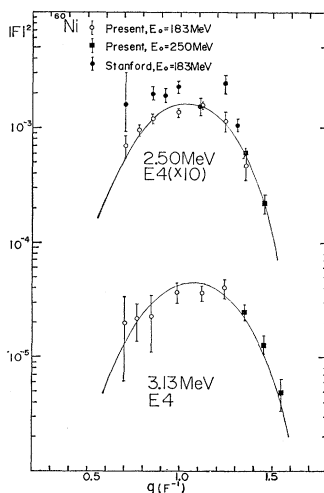


FIG. 8. Experimental $|F|^2$ versus q for the 2.50- and 3.13-MeV excitations. See caption to Fig. 5.

TABLE II. Inelastic form factors for ^{60}Ni at the incident energy of 250 MeV.

E_x (MeV)	J^π	66.3°	72.1°	$10^4 F ^2$ 77.4°	82.2°
1.33	2 ⁺	1.33±0.12	1.44±0.12	1.55±0.15	1.11±0.13
2.16	2 ⁺				
2.50	4 ⁺	0.62±0.06	0.21±0.04		
3.13	4 ⁺	0.25±0.04	0.12±0.02	0.52±0.16	
3.67	4 ⁺	0.60±0.06	0.27±0.05	0.30±0.05	
4.04	3 ⁻	0.58±0.06	0.16±0.03	0.27±0.05	0.30±0.05
4.85	(2 ⁺ , 4 ⁺)				
5.05	4 ⁺ , 6 ⁺	2.15±0.17	1.52±0.10	1.27±0.10	0.99±0.13
5.05	6 ⁺	1.33±0.17	1.12±0.10	1.11±0.10	0.95±0.13
6.20	3 ⁻				
6.85	(2 ⁺ , 5 ⁻)	0.54±0.15	0.41±0.15	0.41±0.18	0.28±0.14
7.05	3 ⁻				

given by the expression

$$B(EL) = \beta_L (Z^2/4\pi) (R/\gamma)^{2L} e^2 F^{2L}. \quad (3)$$

The electromagnetic transition strength G , which estimates the collective character of nuclear state, is given in Weisskopf single-particle units by

$$G = B(EL)/B(EL)_{sp},$$

where

$$B(EL)_{sp} = [(2L+1)/4\pi] [3/(L+3)]^2 R_0^{2L} e^2 F^{2L},$$

with $R_0 = 1.20A^{1/3}$ F.

The values of $B(EL)$ extracted from the present study are given in Table III with the corresponding values of the G for each transition.

III. DISTORTED-WAVE ANALYSIS

A distorted-wave analysis of the form factor for inelastic electron scattering has been developed by a

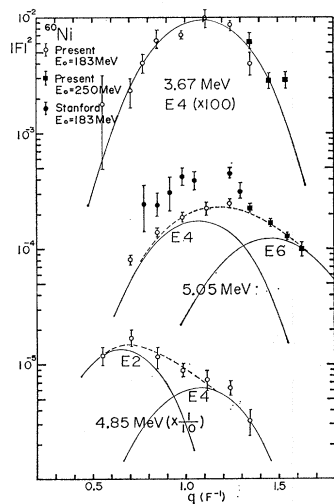


FIG. 9. Experimental $|F|^2$ versus q for the 3.67-, 4.85-, and 5.05-MeV excitations. The $|F|^2$ of 5.05 MeV were decomposed to $E4$ and $E6$ by the help of theoretical curves of Eq. (2) in the text. The $|F|^2$ of 4.85 MeV are tentatively decomposed to $E2$ and $E4$ as mentioned above.

Duke University group, and the analysis of the present experimental data was carried out with the help of the Duke program.²³ In the present calculation, the ground-state charge distribution is taken as a Fermi distribution,

$$\rho(r) = \rho_0 \left[1 + \exp\left(\frac{r-c}{t/4.4}\right) \right]^{-1}, \quad (4)$$

where c is the half-density radius, and t is the skin thickness measured between the 90 and 10% points. In the Duke program one takes the transition charge density as

$$\rho_L(r) = Nr^{L-1} [d\rho(r)/dr], \quad (5)$$

where N is normalization factor, and L is the multipole order. The transition charge density given by Eq. (5) is related to that of Tassie's liquid-drop model.²⁴ The calculated q dependencies of the form

TABLE III. Summary of spins, parities, and reduced transition probabilities in ^{60}Ni extracted from present (e, e') reaction.

E_x (MeV)	J^π	$B(EL)$ ($e^2 F^{2L}$)	$G(B/B_{sp})$	$R(F)^a$
1.33	2 ⁺	$(7.66 \pm 0.77) \times 10^2$	11.0	4.73
2.16	2 ⁺	$(1.5 \pm 0.4) \times 10^1$	0.2	4.50
2.50	4 ⁺	$(1.50 \pm 0.30) \times 10^5$	4.8	4.96
3.13	4 ⁺	$(3.09 \pm 0.62) \times 10^4$	1.0	4.73
3.67	4 ⁺	$(5.67 \pm 1.13) \times 10^4$	1.8	4.62
4.04	3 ⁻	$(1.65 \pm 0.25) \times 10^4$	11.1	4.73
4.85	(2 ⁺)	$(5.0 \pm 1.0) \times 10^1$	0.7	4.73
4.85	(4 ⁺)	$(4.38 \pm 0.88) \times 10^4$	1.4	4.73
5.05	4 ⁺	$(1.22 \pm 0.24) \times 10^5$	3.9	4.73
5.05	6 ⁺	$(1.54 \pm 0.46) \times 10^8$	11.6	4.73
6.20	3 ⁻	$(2.20 \pm 0.33) \times 10^8$	1.5	4.50
6.85	(2 ⁺)	$(3.88 \pm 0.58) \times 10^1$	0.6	4.73
6.85	(5 ⁻)	$(3.53 \pm 0.88) \times 10^9$	5.5	4.96
7.05	3 ⁻	$(2.17 \pm 0.33) \times 10^8$	1.5	4.50

^a g is assumed to be 0.95 F.

²³ S. T. Tuar, L. E. Wright, and D. S. Onley, Nucl. Instr. Methods **60**, 70 (1968).

²⁴ L. J. Tassie, Australian J. Phys. **9**, 407 (1956).

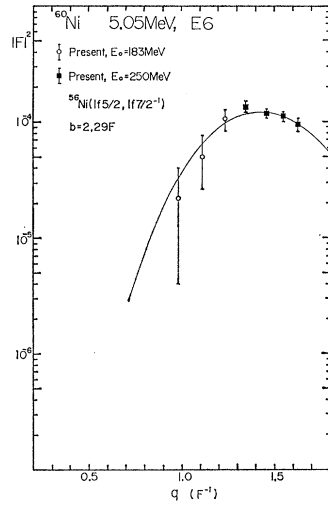


FIG. 10. Experimental $|F|^2$ of 6^+ state at 5.05 MeV. The solid curve is calculated $|F|^2$ of a 6^+ state in ^{60}Ni , assuming a configuration of $(1f_{5/2}, 1f_{7/2}^{-1})$, where oscillator length parameter was taken as $b=2.29\text{ F}$. See the text.

factors of the 1.33-MeV (2^+) and the 4.04-MeV (3^-) states are shown in Figs. 11 and 12 along with experimental data. As can be seen in these figures, the first maximum of the data is well reproduced by the theoretical curve, but does not fit the second one. The comparison of the $B(EL)$ values extracted from the distorted-wave calculation with those of the Born approximation is shown in Table IV. Although the $B(EL)$ values calculated with the distorted-wave and the Born approximation are in reasonable agreement for the 2^+ state, serious discrepancies are seen for those of the 3^- and 4^+ states as shown in Table IV. The $B(EL)$ values of distorted-wave calculation of

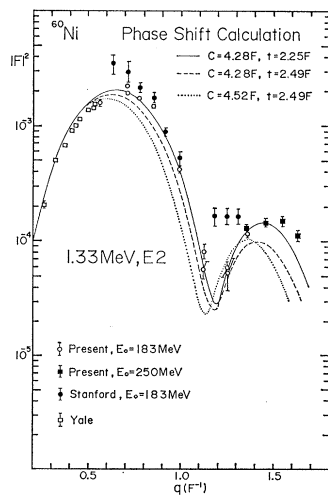


FIG. 11. Theoretical and experimental $|F|^2$ versus q for the 1.33-MeV (2^+) state. The theoretical curves were calculated by the Duke program of distorted-wave analysis (see Ref. 23) using three sets of parameters.

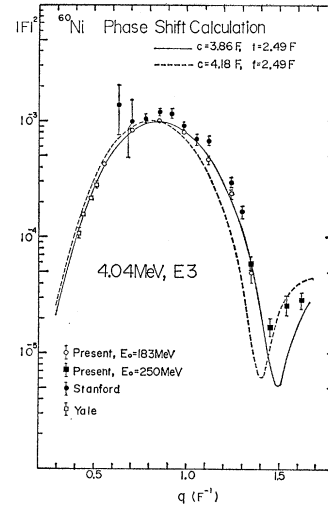


FIG. 12. Theoretical and experimental $|F|^2$ versus q for the 4.04-MeV (3^-) state. The curves were calculated by the Duke program.

3^- and 4^+ states are about 1.7 and 3.1 times greater than those of Born approximation, respectively.

The definite origins of these discrepancies are not known at present; however, the values of $B(EL)$ extracted from the experimental form factors with Born approximation will be used in the following discussions and comparisons with the other experimental results and the theoretical predictions.

IV. DISCUSSION AND COMPARISON WITH THEORY

The form factors which were obtained by the previous electron scattering measurements at 183 MeV taken at Stanford are plotted in Figs. 5, 6, 8, and 9. For the form factors of the 1.33- and 4.04-MeV excitations, the present results are consistent with the data of Stanford within the experimental errors. In the comparison with those of the 2.50- and 5.05-MeV excitations, the agreement is not very good. In order to compare the present data with those obtained at Yale,² at 45–65 MeV, the Yale form factors were adjusted to take account of the difference of bombarding energy with the help of the distorted-wave calculation.²³ The results are plotted in Figs. 5 and 6. Although

TABLE IV. Comparison of reduced transition probabilities in the Born approximation with those of distorted-wave calculation.

E_x (MeV)	J^π	$B(EL)$	
		Born approximation	Distorted-wave calculation
1.33	2^+	7.66×10^2	9.92×10^2
2.50	4^+	1.50×10^5	4.63×10^5
4.04	3^-	1.65×10^4	2.78×10^4

TABLE V. Values of transition probabilities in single-particle units (G) for ^{60}Ni extracted from present and previous measurements.

E_x (MeV)	J^π	Present	(e, e') ^a	(e, e') ^b	(p, p') ^c	(p, p') ^d	(p, p') ^e	(p, p') ^f	(C.E.) ^g	(γ, γ) ^h
1.33	2 ⁺	11.0	12	17.1	21	19.5-28.1	12	15.1	13	12.5
2.16	2 ⁺	0.2			1.4					
2.50	4 ⁺	4.8		3.62						
3.13	4 ⁺	1.0								
3.67	4 ⁺	1.8								
4.04	3 ⁻	11.1	19	15.9	14	12.8-15.5	8.8	9.3		
4.85	(2 ⁺)	0.7								
4.85	(4 ⁺)	1.4								
5.05	4 ⁺	3.9		4.9			5.2	5.7		
5.05	6 ⁺	11.6								
6.20	3 ⁻	1.5			7		2.0			
6.85	(2 ⁺)	0.6			($E_x=6.21$ MeV)					
6.85	(5 ⁻)	5.5			7					
7.05	3 ⁻	1.5			($E_x=7.12$ MeV)					

^a Reference 2.^b Reference 1.^c Reference 5.^d Reference 4.^e Reference 3.^f Reference 6.^g Coulomb excitation, P. H. Stelson and F. K. McGowan, Nucl. Phys. 32, 652 (1962).^h F. R. Metzger, Phys. Rev. 103, 983 (1956).

the ranges of q do not overlap, the curves which represent the best fit to the present data are also consistent with those of Yale. The levels with J^π of 2⁺ at 1.33 MeV, 2⁺ at 2.16 MeV, 4⁺ at 2.50 MeV, 3⁻ at 4.04 MeV, and 4⁺ at 5.05 MeV, are well known from previous studies. The presence of a 3⁻ state at 6.2 MeV was first reported by Koike *et al.*³ using the (p, p') reaction. Ballini *et al.*^{5,25} also suggested the presence of high-lying 3⁻ states at 6.21 and 7.12 MeV, to which the present 6.20- and 7.05-MeV excitations may correspond. The 6.20- and 7.05-MeV excitations were confirmed as $J^\pi=3^-$ in this experiment. Levine *et al.*²⁶ and Shafroth *et al.*²⁷ from measurements of a $(\gamma-\gamma)$ correlation following the decay of ^{60}Cu , and Sen Gupta *et al.*²⁸ and Mohindra *et al.*²⁹ from $^{60}\text{Ni}(p, p'\gamma)$ γ -ray angular distribution, have uniquely identified the 3.12-MeV state as a 2⁺. This state presumably corresponds to the 3.13-MeV peak observed in the present (e, e') reaction. However, it can be seen in Fig. 8 that the q dependence of $|F|^2$ for the 3.13-MeV peak is reproduced well with the theoretical curve assuming a spin of 4⁺. Very recently, Inoue³⁰ has reported that the angular distribution of the $^{60}\text{Ni}(\alpha, \alpha')$ reaction for the 3.11-MeV peak seems to have a contribution due to a 4⁺ state. There may be a 2⁺ state at 3.12 MeV, but it would be weakly excited in the present

reaction. Jolly³¹ has reported a slightly enhanced ($G=3$) 3⁻ state at 3.13 MeV from the analysis of the angular distribution of the $^{60}\text{Ni}(d, d')$ reaction. However, the possibility of such a state may be ruled out by the results of the present experiment. Inoue³⁰ has suggested there may be a 4⁺ state at 3.70 MeV, from $^{60}\text{Ni}(\alpha, \alpha')$ reaction; this may correspond to the 4⁺ at 3.67 MeV found in the present experiment.

The 2⁺ state at 2.16 MeV and the 4⁺ state at 2.50 MeV have been supposed to be members of the "two-phonon" triplet. The experimental angular distributions of (p, p') ⁵ and (α, α') ⁹ reactions for these states have been rather poorly reproduced by the DWBA calculation based on the one-phonon vibrational model. In the case of the (e, e') reaction, however, fits to the q dependence of the form factors for these "two-phonon" states have been obtained using Eq. (2), and are equally as satisfactory as fits obtained for the other states. From these results it could be concluded that the excitation of these states by electrons must proceed by a simple mechanism, which is not the case for true two-phonon states. The comparison of (e, e') with the other charged-particle reactions may lead to better understanding of the excitation mechanism. The important 0⁺ state at 2.29 MeV which was reported from (α, α') ⁹ and (p, p') ⁵ reactions was not observed in the present (e, e') experiment; the reason for this will be discussed later.

The values of the reduced transition probabilities in Weisskopf units extracted from the previous (e, e') and the other reactions are summarized for comparison with the present results in Table V. The present

²⁵ R. Ballini, N. Cindro, J. Delaunay, J. Fouan, M. Loret and J. P. Passerieux, Phys. Letters 21, 708 (1966).²⁶ N. Levine, H. Frauenfelder, and A. Rossi, Z. Physik 151, 241 (1958).²⁷ S. M. Shafroth and G. T. Wood, Phys. Rev. 149, 827 (1966).²⁸ A. K. Sen Gupta and D. M. Van Patter, Phys. Letters 3, 355 (1963).²⁹ R. K. Mohindra and D. M. Van Patter, Phys. Rev. 139, B274 (1965).³⁰ M. Inoue, Nucl. Phys. A119, 449 (1968).³¹ R. K. Jolly, Phys. Rev. 139, B318 (1965).

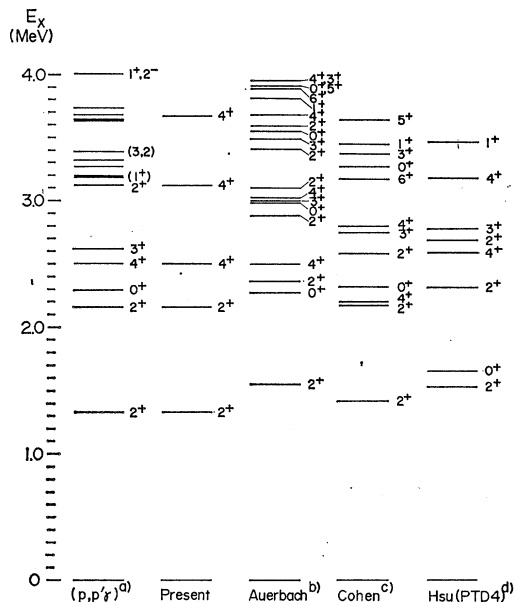


FIG. 13. Experimental and calculated energies of low-lying positive parity states in ^{60}Ni . (a) Ref. 27 and 29, (b) Ref. 14, (c) Ref. 13, and (d) Ref. 16.

values are in excellent agreement with those of (p, p') reactions of Refs. 3 and 6. The value of $G=4.8$ at the 2.50-MeV state agrees with the estimate of Morinaga and Takahashi,³² which was derived from the measurement of the branching ratio of the direct ground-state transition from the 2.50-MeV state, to the cascade transition.

The low-lying even-parity states observed in the present study are shown in column 2 of Fig. 13; column 1 shows states which have been found in previous experiments.^{27,29} The 3^+ state should be excited by electron spin-flip process, and may not be observed in the present experiment, which was carried out at relatively forward angles.

Recently, detailed shell-model calculations were performed for Ni isotopes by Cohen, Lawson, Macfarlane, Pandya, and Soga,¹⁸ and by Auerbach.¹⁴ In both calculations, only neutrons in the $2p_{3/2}$, $1f_{5/2}$, and $2p_{1/2}$ orbits were considered to contribute to the low-lying states of the Ni isotopes. The effective interactions were deduced from a least-squares fit to the observed energy spectra of the Ni isotopes. The calculated energies of ^{60}Ni taken from Refs. 13 and 14 are shown in columns 3 and 4 of Fig. 13. Hsu¹⁶ also performed a calculation of the spectra and transition probabilities for the Ni isotopes, and compared the results of a standard shell-model calculation with other approximation methods. The calculated energies which are based on a number-projected Tamm-Dancoff approxi-

mation (PTD4) are shown in column 5 of Fig. 13. The energies of 4^+ states predicted by the theories of Auerbach, of Cohen *et al.*, and of Hsu are very close to the results of the present experiment as can be seen in Fig. 13.

The phenomenological vibrational model predicts an inhibition for the cross-over transitions $2_2^+ \rightarrow 0_1^+$ and $4_1^+ \rightarrow 0_1^+$. The selection rule follows from the fact that these transitions, according to the vibrational model, are due to a "two-phonon" transfer. Recent calculations of Cohen *et al.*¹⁸ and of Auerbach¹⁴ do not support this argument. These authors found the 2_2^+ state and also the 4_1^+ state of Ni isotopes to be predominantly seniority-2 configurations, while "two-phonon" states have large seniority-4 components. The present experimental results seem to support this interpretation, since the $0_1^+ \rightarrow 4_1^+$ excitation has collective strength. Recent theoretical work of Yamamura, Tokunaga, and Marumori³³ has also shown that the concept of the "two-phonon" state based on the RPA breaks down for ^{60}Ni .

The $E2$ transition probabilities of ^{60}Ni are calculated using an effective charge for the neutron.^{13,14,16} The calculated and experimental values of $B(E2; 0_1^+ \rightarrow 2_1^+)$ and $B(E2; 0_1^+ \rightarrow 2_2^+)$ are given in the Table VI. The agreement between theory and experiment is satisfactory. Cohen *et al.*¹⁸ have suggested that the 2_3^+ state in Ni isotopes is characteristic of the strong mixing in seniority. The third 2^+ state in ^{60}Ni may correspond to the 2^+ state at 3.12 MeV, hardly observed in the present (e, e') reaction, as discussed earlier in this section.

Hsu and French¹⁵ and Hsu¹⁶ have suggested that the quasiparticle picture is not suitable to describe the triplet member of the "two-phonon" state in the TD4 approximation; on the other hand, in the particle picture, the 0^+ and 2^+ members can be identified with the 0_2^+ and 2_2^+ shell-model states, while the strength of the 4^+ member is distributed between the 4_1^+ and 4_2^+ shell-model states. If the actual states of ^{60}Ni could be described by those of shell model, this interpretation would be supported by the present experimental results as follows: (a) $B(E4; 0_1^+ \rightarrow 4_1^+)$ and

TABLE VI. Calculated and experimental reduced transition probabilities (in units of e^2F^4) for the first and second 2^+ states in ^{60}Ni .

	Auerbach ^a	Hsu ^b	Present
$0_1^+ \rightarrow 2_1^+$ (1.33 MeV)	1001.31	922.5	766 ± 77
$0_1^+ \rightarrow 2_2^+$ (2.16 MeV)	30.43	10.65	15 ± 4

^a Reference 14.

^b Reference 16.

³² H. Morinaga and K. Takahashi, J. Phys. Soc. Japan **14**, 1460 (1959).

³³ M. Yamamura, A. Tokunaga, and T. Marumori, Progr. Theoret. Phys. (Kyoto) **37**, 336 (1967).

$B(E4; 0_1^+ \rightarrow 4_2^+)$ are estimated to be $G=5$ and 1, respectively, (b) $B(E2; 0_1^+ \rightarrow 2_2^+)$ is very weak, and (c) $B(E0; 0_1^+ \rightarrow 0_2^+)$ is hardly observed.

Cohen *et al.*¹³ and Auerbach¹⁴ have suggested that 0_1^+ and 0_2^+ states in even- A Ni isotopes have predominantly seniority 0, and the experimental inhibition of the $0_1^+ \rightarrow 0_2^+$ excitation discussed above, may be expected from the seniority number, since the transition from a state of seniority 0 to another state of seniority 0 seems to be forbidden by the simple mechanism in electroexcitation. The inhibition of $2_2^+ \rightarrow 0_1^+$ transition can also be understood from the arguments of Cohen *et al.*¹³ and of Auerbach,¹⁴ because the 2_1^+ state is well reproduced by the action of the quadrupole operator Q^2 on the ground-state wave function, and little of the available $E2$ strength is left for the cross-over transition $2_2^+ \rightarrow 0_1^+$. Their interpretation for the $4_1^+ \rightarrow 0_1^+$ transition was already mentioned above.

The existence of more than one octupole state in the ^{60}Ni is very interesting, and they cannot be interpreted in the simple vibrational model. Theoretical work based on the quasiparticle model has been performed for the octupole states by Veje.³⁴ He has suggested that the octupole vibrations are less collective than the quadrupole ones, and the oscillator strength might spread over the several states. For the Ni isotopes, Veje further mentioned that the lowest octupole states are essentially governed by the strong neutron transition $p_{3/2} \rightarrow g_{9/2}$ and the weak $f_{5/2} \rightarrow g_{9/2}$ transition, the most important proton excitation being $f_{7/2} \rightarrow g_{9/2}$, which is of medium strength; the proton transitions from the sd shell are rather weak and not very low in energy. The results calculated by Veje show the presence of some octupole states other than the one prominent state for the Ni isotopes. Comparison of theoretical and experimental energies of 3^- states are shown in Table VII. The values of $B(EL)$ for $E3$ transitions of ^{60}Ni have been calculated by Veje³⁴ and by Yoshida³⁵; the theoretical and the present experimental values of $B(EL)$ are also listed in Table VII. The agreement between the experimental and theoretical results is satisfactory.

A striking feature of the 5.05-MeV (6^+) state is its collective nature which has the value of $G=11.6$. The collective states in ^{60}Ni are composed of off-shell neutron configurations as mentioned above,^{13,16,34} or made up of a linear combination of many particle-hole states. The 5.05-MeV (6^+) state which is char-

TABLE VII. Calculated and experimental reduced transition probabilities (in units of $10^4 e^2 P^6$) for the excited octupole states in ^{60}Ni .

Veje ^a		Yoshida ^b		Present	
E_x (MeV)	B	E_x (MeV)	B	E_x (MeV)	B
4.07	3.9	4.08	2.3	4.04	1.65 ± 0.25
6.25	0.6			6.20	0.22 ± 0.04
7.30	3×10^{-2}			7.05	0.21 ± 0.03

^a Reference 34.

^b S. Yoshida, Nucl. Phys. **38**, 380 (1962).

acteristic of the high-spin value, is assumed to be built on a simple proton particle-hole configuration ($1f_{5/2}, 1f_{7/2}^{-1}$). However, the calculation of particle-hole states in ^{60}Ni cannot be carried out in a straightforward fashion, because of the complication of off-shell neutrons in the $2p_{3/2}$ orbit. The present experimental form factor of the 5.05-MeV (6^+) state may be compared with theoretical calculations of the 6^+ state in ^{56}Ni , which is the core of ^{60}Ni , assuming a pure ($1f_{5/2}, 1f_{7/2}^{-1}$) configuration. The calculated result is shown in Fig. 10 as a solid line. It can be seen that the absolute value of the theoretical curve for ^{56}Ni fits completely the experimental data of ^{60}Ni , where the length parameter of the harmonic oscillator wave function is determined to be $b=2.29$ F.

The q dependence of $|F|^2$ of a 5^- state in ^{56}Ni was also calculated assuming a ($1g_{9/2}, 1f_{7/2}^{-1}$) configuration to compare that with the experimental $|F|^2$ of the 6.85-MeV (5^-) state in ^{60}Ni . The calculated result is in absolute agreement with the experimental data if the value of $b=2.30$ F is used.

Further investigations of 5^- and 6^+ states in Ni isotopes may extract oscillator length parameters for the $1f$ -shell wave functions, and their dependence on off-shell neutron number.

ACKNOWLEDGMENTS

The authors wish to thank Professor S. Fujii, Professor H. Ui, and Professor T. Sasakawa for their valuable discussions and advice. They also thank Professor K. Shoda and Professor M. Sugawara, who were primarily responsible for the construction of the beam transport system and the spectrometer magnet. They are also indebted to Professor D. S. Onley and Professor L. E. Wright who kindly sent them a distorted-wave computer program. They are grateful to the accelerator crew for beam operation during the extended periods of measurements.

³⁴ C. Veje, Kgl. Danske Videnskab. Selskab, Mat.-Fys. Medd. **35**, No. 1 (1966).

³⁵ S. Yoshida, Nucl. Phys. **38**, 380 (1962).